Desalination and Water Treatment
www.deswater.com
doi: 10.1080/19443994.2015.1095682

57 (2016) 19149–19159
September

Taylor & Francis
Taylor & Francis Group

Desalinated seawater into pilot-scale drinking water distribution system: chlorine decay and trihalomethanes formation

Xunchao Li, Cong Li*, Mingda Bayier, Taotao Zhao, Tuqiao Zhang, Xinbo Chen, Xinwei Mao

College of Civil Engineering and Architecture, Zhejiang University, Hangzhou 310027, China, email: lixunchao@zju.edu.cn (X. Li), Tel./Fax: +86 571 87952015; congil@zju.edu.cn (C. Li), 18868817521@163.com (M. Bayier), zttxzfx2008@126.com (T. Zhao), ztq@zju.edu.cn (T. Zhang), cxbgzw0901@163.com (X. Chen), catum@163.com (X. Mao)

Received 17 March 2015; Accepted 12 September 2015

ABSTRACT

Residual chlorine decay and trihalomethanes (THM) formation of desalinated seawater by ultrafiltration (UF) and nanofiltration (NF) membranes in a pilot-scale water distribution system (DWDS) were investigated. Three-dimensional fluorescent features of two source waters including NF permeate and municipal water were studied. Sixteen groups of datasets were obtained to explore the effects of initial chlorine concentration (ICC), dissolved organic carbon (DOC), and temperature on chlorine decay and THM formation in laboratory conditions and pilot-scale DWDS, respectively. A first-order model was applied to evaluate the chlorine decay of desalinated seawater and a new model combining ICC, DOC concentration, and temperature was obtained to determine the first-order decay coefficient. Other seven models describing the kinetics of chlorine decay were also applied and compared in this study. Total trihalomethanes (TTHM) formation kinetics was studied and first-order model was suggested to describe this formation. The relationship between TTHM formation and chlorine demand was demonstrated and the results showed that second-order polynomial model better described the relationship.

Keywords: Desalinated seawater; Pilot-scale drinking water distribution system (DWDS); Chlorine decay; Trihalomethanes (THM) formation

1. Introduction

Global water shortage (both in the quantity and quality) is increasingly becoming a challenge, affecting human health and sustainable economic development around the world. Such problem prompts many governments and investors to take a look at seawater desalination with its cost decreasing [1]. Seawater desalination offers a seemingly unlimited, steady supply of high-quality water to alleviate the pressure for water-stressed countries, without impairing natural freshwater ecosystems in water supply [2]. Desalinated seawater is becoming an important and feasible resource for drinking water production and it is highly expected to make up for the great freshwater shortfall by partially substituting for traditional resources such as lakes, rivers and groundwater [3]. Currently, among various desalination technologies available, reverse osmosis and nanofiltration membrane technology are becoming the leading

---

*Corresponding author.

technologies for new desalination installations [4]. Since reverse osmosis cannot be used for partial and/or selective demineralization of salty solutions, nanofiltration (NF, known as low-pressure reverse osmosis) is more suitable for producing drinking water directly without the need for remineralization [5]. Treated seawater from NF desalination plants vary in quality from treated freshwater in some respects; such as pH, salinity, total dissolved solid (TDS), hardness, conductivity, halide ions, ammonia, sulfide, micro-organisms, and dissolved natural organic matter (DNOM). Furthermore, before being integrated into the existing drinking water distribution system (DWDS), desalinated seawater should be disinfected to kill or inactivate pathogenic micro-organisms to meet the standards for drinking. However, little researches have been as yet reported on the desalinated seawater chlorination and its mechanism when being integrated into the existing DWDS.

Chlorine is used worldwide as a disinfectant in continuous water supply owing to its low cost, high efficiency, and can be maintained in the DWDS for a considerable period of time. As chlorine is transported through the pipe networks in a distribution system, it can react with a variety of substances both within the bulk water and from the pipe wall [6,7], thus causing the loss of chlorine, referred to as chlorine decay [8,9]. Chlorine is lost by its reaction with substances remaining in the water after treatment, not only with micro-organisms but also with DNOM, halide ions, ammonia, iron, and manganese [10]. Therefore, to maintain a nominated residual chlorine concentration throughout the distribution system even at extremities, secondary disinfection (rechlorination) may be required to limit the regrowth of micro-organisms. However, a higher initial chlorine concentration (ICC) than necessary may result in taste and odor problems to upstream consumers and/or disinfection byproducts (DBPs), which are reportedly of significant health risk (teratogenicity, genotoxicity, and carcinogenicity) to humans [11–15]. Trihalomethanes (THM, including chloroform, TCM; bromodichloromethane, BDCM; dibromochloromethane, DBCM; bromoform, TBM), and haloacetic acids (HAAs) are the two most prevalent classes of DBPs in chlorinated drinking water [16], and are regulated in some countries around the world (e.g. USEPA and China) [17–19]. The maximum concentration of total trihalomethanes (TTHM), the sum of the concentrations of above four chemicals, is 0.32 mg/L according to the Drinking Water Standard of China [19,20]. Therefore, more attention should be given to desalinated seawater chlorination and its mechanism of chlorine decay and DBPs formation in the DWDS.

In this study, desalinated seawater collected from an UF/NF desalination plant was injected into a pilot-scale DWDS and then circulated in a pipe network. The purpose of the study was to (1) measure the initial characteristics of desalinated seawater in comparison with surface freshwater, particularly in the characterization of organic species; (2) to describe the mechanism and a kinetic model of chlorine decay based on the pilot-scale DWDS; (3) to evaluate THM formation. This work provides information on chlorination of desalinated seawater in DWDS to assist water supply regulators.

2. Materials and methods

2.1. Reagents

A mixture of four THM (TCM, DCBM, DBCM, and TBM) standards, 2,000 μg/mL in methyl tert-butyl ether (MTBE), was purchased from Supelco (PA, USA). Sodium thiosulfate, phosphate buffer, sodium hydroxide and sodium hypochlorite (analytical reagent, 10% active chlorine) were all obtained from Aladdin in Shanghai. The ultrapure water employed in the experiments for preparing solutions and rinsing glassware had been distilled and then passed through a Milli-Q water purification system (Heal Force, Electrical resistivity >18 MΩ cm).

2.2. Analytical methods

Residual chlorine (free chlorine) was measured by a residual chlorine comparator (HACH DR2800 accompanied with powder package), which was regularly calibrated by the DPD method. The concentration of bromide ion was analyzed using an ion chromatograph (ICS-2000, Dionex). Dissolved organic carbon (DOC) of water samples pre-filtered through a 0.45-μm membrane was measured using TOC analyzer (Shimadzu TOC-V CPH). pH was determined using a pH electrode from Thermo Scientific, dissolved oxygen (DO) was measured by an InoLab Oxi730, conductivity was determined by HACH DR-2000, and hardness by EDTA titrimetric method.

The organic species of water samples, pre-filtered through a 0.22-μm membrane, were characterized by 3D fluorescence spectrometer (FluoroMax-4, Horiba Jobin Yvon Inc., USA) in synchronous-scan excitation modes. The analytical parameters of the 3D fluorescence spectrometer are as follows: the excitation source, 150 W Xenon lamp; excitation wavelength range, 220–400 nm; emission wavelength range, 250–600 nm.

The concentrations of THM in the water samples were determined by headspace analysis by a gas chromatograph (Varian GC-450) equipped with an electron capture detector (ECD) and 15 m × 0.25 mm × 0.25 μm column (Agilent HP-5), and detection limits of THM were less than 0.1 μg/L at a GC-ECD operating condition of detector 300℃, injector 150℃ [21]. The chromatographic peaks of THM were confirmed by GC–MS analysis (Shimadzu-QP2010 Plus) equipped with a Purge & Trap Sample concentrator (Atomx, Teledyne Tekmar, USA).

2.3. Experimental waters and conditioned pilot-scale DWDS

2.3.1. Experimental waters

Experimental waters were sourced from two water treatment plants: (1) municipal water in Hangzhou City, transported from a conventional treatment plant with the Qiantang River as surface water source; (2) desalinated seawater treated by an UF/NF desalination plant. In this plant, the pre-treatment process followed by NF membrane filtration was conventional pre-disinfection/flocculation/coagulation/multimedia filtration and UF membrane filtration to remove excessive turbidity, suspended solids, micro-organisms, organic matters, and minerals.

In the phase of initial water quality evaluation, and for better comparison, three kinds of water samples were collected to evaluate their initial characteristics: the first one was from a municipal water supply, the second one was UF permeate (obtained after the UF filtration unit), and the last one was NF permeate (obtained after the NF filtration unit). All water samples were analyzed three times.

For chlorine decay and THM formation experiments, municipal water and NF permeate were adjusted to pH 7.5 ± 0.1 by phosphate buffer, and then pumped into the pilot-scale DWDS at Zhejiang University.

2.3.2. The conditioned pilot-scale DWDS and operation

The pilot-scale distribution network used in this study consisted of a ductile iron pipe loop of approximately 80 m length and 150 mm diameter and some other accessories such as heat exchanger and so on, as shown in Fig. 1. Experimental waters were circulated in the pipe. Water temperature and velocity were managed by automatic control system. Before pumping experimental water into the loop, the pipe was washed for 20 min.

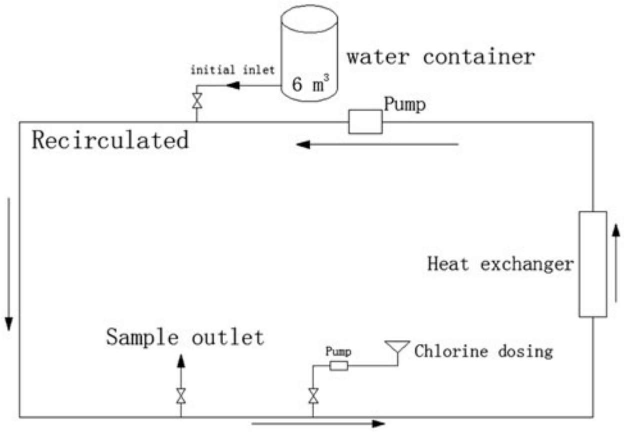

Fig. 1. Schematic representation of a loop of the pilot-scale DWDS.

In order to investigate the kinetics of chlorine decay and THM formation in different waters, predetermined amount of sodium hypochlorite were added by the equipment of chlorine dosing and then mixed with waters to set ICC as two levels, 3.5 and 0.4 mg/L, respectively. The flow velocity was maintained as 1 m/s and water temperature was set at 10 and 20℃ during the experimental period. Water samples were collected and analyzed at 0.1, 0.2, 0.5, 1, 1.5, 2, 3, 4, 6, 8, and 10 h. Samples for THM determination were added excessive sodium thiosulfate solution to consume residual chlorine.

3. Results and discussions

3.1. The characteristics of waters

3.1.1. Standard water quality parameters

Water quality data of the two finished waters are presented in Table 1. Residual chlorine concentration in the municipal water and NF permeate was initially negligible.

3.1.2. Fluorescence properties

Chlorine reacts with DNOM, which leads to chlorine decay and formation of numerous DBPs such as THM. However, natural organic matter (NOM) is a complex heterogeneous mixture composed of humic acids, fulvic acids, low-molecular weight organic acids, carbohydrates, proteins, and other compound classes [22]. Different NOM fractions vary in the reactivity with chlorine and result in different DBP formation, in species and concentrations. Platikanov et al. [23] found that DNOM fractions could affect the THM

Table 1
Water quality parameters of the experimental waters

Water samples	Municipal water	UF permeate	NF permeate
pH[a]	7.5 ± 0.1	7.5 ± 0.1	7.5 ± 0.1
DO (mg/L)	5.24	8.36	8.42
Conductivity (μs/cm)	267.0	784.6	198.8
Hardness (mg/L)	74.54	80.53	25.22
TDS (mg/L)	175.3 ± 1.5	585.2 ± 1.2	189.4 ± 0.4
Total NH_3-N (mg/L)	≤0.3	N.D.[b]	N.D.[b]
DOC (mg/L)	5.87 ± 0.14	3.34 ± 0.06	2.67 ± 0.03
Br^-(mg/L)	0.06	27.65	1.39
Nitrite (mg/L)	<0.01	<0.01	<0.01
Free chlorine (mg/L)	<0.02	0.00	0.00

[a] pH value of above waters was adjusted by phosphate buffer.
[b] N.D. means not detected.

formation, and their work revealed that colloidal fraction has a relatively low contribution to THM formation; transphilic fraction was responsible for about 50% of the chloroform formation, and the hydrophobic fraction was the most important to the brominated THM formation. Therefore, a better understanding of the properties of NOM would greatly improve our understanding of the underlying mechanisms responsible for chlorine decay model and DBP formation.

Over the past few decades, many researchers [24–26] have reported that fluorescence techniques are suitable for the characterization and structural properties of DNOM both in natural fresh and oceanic water samples. In this study, three-dimensional excitation–emission matrices spectroscopy was applied to characterize the chemical and physical properties of DNOM in the experimental waters. Based on the most common fluorescent peaks (fluorophores) of dissolved organic matter in different aquatic environments (listed in Table 2) and Parallel factor analysis (PARAFAC) model [26,27], the fluorescence properties of municipal water, UF permeate, and NF permeate were compared.

EEM fluorescence spectrograms (contour EEM plots and fluorescence intensity) of DNOM in municipal water, UF permeate, and NF permeate are shown in Fig. 2. One maximum is observed in all three EEMs (Peak A_1, B_1, C_1 in Fig. 2(a)–(c), respectively), from excitation in the UV region at 270–290 nm. These three peaks have an emission maximum between 320 and 370 nm. These maxima are identified as protein-like fluorophores (see Table 4). However, some minor differences in peak positions and shapes are evident, which indicates that there are some minor differences in protein-like composition between three water samples. EEM peaks (A_1 in Fig. 2(a), B_1 in Fig. 2(b)) are in similar positions of Ex/Em = 285/325 nm, which suggests that they are Peak B (tyrosine-like fluorophore) [24], while peak in Fig. 2(c) has different shape and is shifted 20 nm towards longer wavelengths along the emission axis. This suggests it is peak T (tryptophan-like fluorophore) [27]. Moreover, such three protein-like fluorophores vary in fluorescence intensity with a large gap, namely in the order: municipal water > UF permeate > NF permeate (i.e. 1.493E + 06, 7.425E + 05, 7.146E + 04 cps, respectively), which suggests that

Table 2
Major fluorophores of dissolved organic matters in different aquatic environments. (Previous identified by Coble et al. [24,28,29], Stedmon et al. [27] and Blough and Del Vecchio [30])

Label	Compounds	EX (nm)	EM (nm)
B	Tyrosine-like, protein-like	275	310
T	Tryptophan-like, PROTEIN-like	275	340
A	Ultraviolet humic-like	260	380–460
C	Visible humic-like	350	420–460
M	Marine humic-like	312	380–420
P	Chlorophyll	400	660
N	Unknown (associated with biologic productivity)	280	370–375

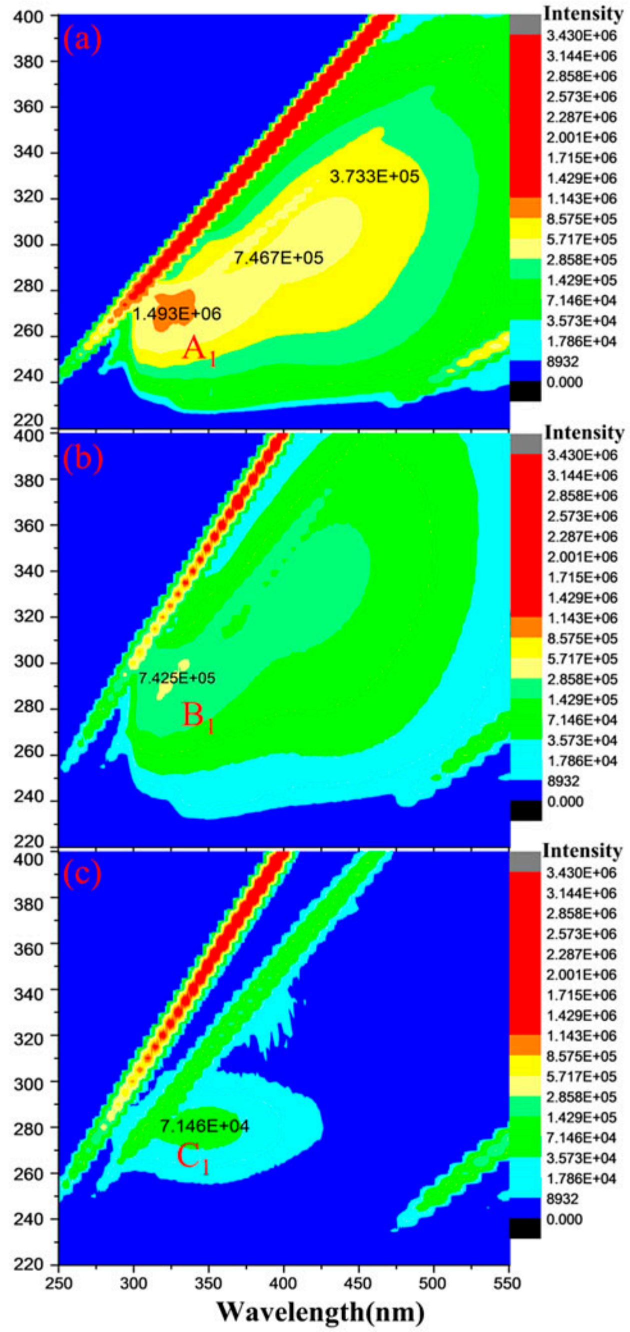

Fig. 2. EEM fluorescence spectrograms (contour EEM plots and fluorescence intensity). (a) Municipal water, (b) UF permeate, and (c) NF permeate.

protein-like matter in the three water samples also followed this order. This order corresponds with TOC concentration (Table 2) of each water sample. Humic-like fluorescence was observed in all samples, but only the municipal water sample (Fig. 2(a)) had a very high fluorescence intensity, which indicates that humic-like matter in the municipal water sample accounted for a considerable percentage of the DNOM.

Of note, the differences of DNOM species in the three water samples, in the aspects of protein-like and humic-like matters, could have great influence on chlorine decay and THM formation.

3.2. *Chlorine decay and THM formation*

Management of chlorine concentrations in drinking water supplies is essential feature in ensuring that water is safe and acceptable to the consumer [31]. The multiobjective nature of chlorination, resulting from the tradeoff between disinfection benefits and its side effect such as DBPs, has provided greater motivation to describe chlorine decay and byproduct formation through mathematical models [32].

In this study, the purpose of the modeling was to describe chlorine decay in the pilot-scale DWDS. Eight (two finished waters with two ICCs at two temperatures) sets of chlorine decay data were obtained from laboratory experiments conducted to measure bulk chlorine decay. Another eight sets were obtained from the experiments in the pilot-scale DWDS to measure overall chlorine decay (bulk decay and pipe wall decay) [7].

3.2.1. *Application of first-order model*

A number of studies have been conducted on the development of models to predict chlorine decay in drinking water. The long-term chlorine decay has been typically modeled using first-order exponential kinetics [33]. Many packages such as EPANET program [7] assume that both the overall and bulk decay to be first-order as well.

$$C_t = C_0 \cdot \exp(-k_{\mathrm{b}}t) \qquad (1)$$

where C_t is the chlorine concentration at time t; C_0 is ICC; t is time (h); and k is the first-order reaction rate coefficient (h^{-1}).

Chlorine decay in DWDS of desalinated seawater has as yet seldom been reported. Based on the analysis of water quality characteristics and experimental data acquired, the first-order model was applied to demonstrate chlorine decay of desalinated seawater. The fit values of the curves are shown in Figs. 3 and 4.

It can be seen from Figs. 3 and 4 that, within 10 h of decay time, the decay coefficient of municipal water is higher than that of NF permeate in all experimental conditions. Such differences exist between the

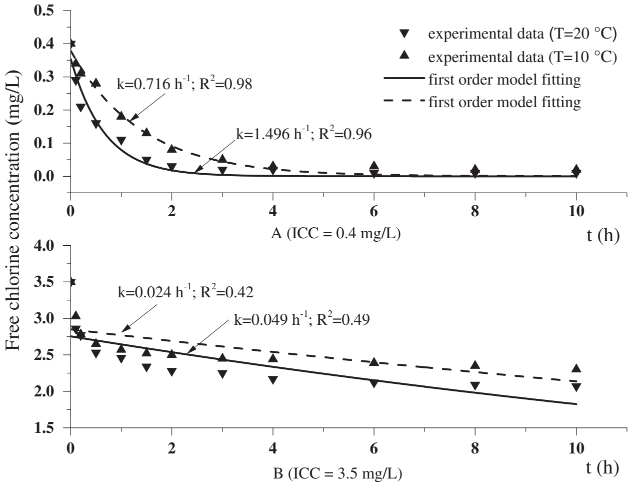

Fig. 3. First-order model fitting of bulk chlorine decay in municipal water.

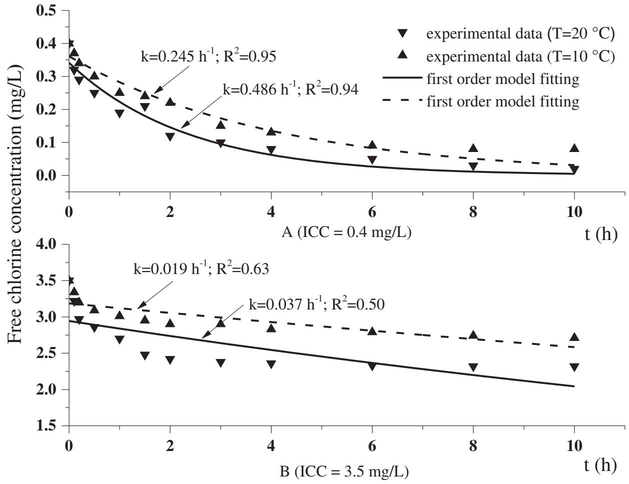

Fig. 4. First-order model fitting of bulk chlorine decay in NF permeate.

municipal water and NF permeate regardless of variations in the experimental conditions such as ambient temperature, ICC, and other factors. This suggests that the only reason leading to the differences is subject to the differences between the quality characteristics of the two initial waters, detailed in Section 3.1. Higher concentrations of water quality parameters such as hardness, Total NH_3-N, and especially DOC in the municipal water than NF permeate appears to affect the chlorine reactivity. The presence of NH_3-N can result in fast reaction with free chlorine and consequently generate chloramines which are well known as bound chlorine. In the municipal water, less than 0.3 mg/L NH_3-N caused a particular amount of chlorine demand, while no NH_3-N was detected in the NF permeate. Moreover, a higher DOC concentration in municipal water would greatly accelerate the oxidation addition and electrophilic substitution reactions with chlorine [10], thus causing more chlorine demand and yielding more DBPs. Not only DOC concentration but also constituent compounds would affect the chlorine reactivity. The presence of humic-like and protein-like matters in municipal water would probably have accelerated the consumption of chlorine. Therefore, such chlorine demand in municipal water would increase chlorine decay and be expressed through a high decay rate coefficient.

3.2.1.1. Factors influencing the bulk decay rate coefficient. The bulk decay rate coefficient (k_b) was found to have significant correlation with temperature, ICC, and organic compounds within the water which is generally measured by TOC [34,35].

The Arrhenius equation has been widely used to describe the way in which temperature changes affect the chemical reactions causing chlorine decay [31].

$$k_b = F \cdot \exp\left(\frac{-E/R}{T+273}\right) \tag{2}$$

where k_b is the first-order reaction rate coefficient (h^{-1}); T is temperature (℃); the value of F and $-E/R$ depends on the reaction. As shown in Table 3, the actual value of $-E/R$ and F in Eq. (2) are numerically calculated and listed.

It has been reported that the first-order decay coefficient has a linear relationship with TOC [36]. Moreover, the effects of temperature and ICC on chlorine decay in different water samples were studied by Hua et al. [34] and the results showed that the decay constants were inversely proportional to ICC.

In this study, an equation combining TOC, ICC, and temperature was assumed and applied here.

$$k_b = \mathrm{TOC}^{\alpha} \cdot \mathrm{Cl}_0^{\beta} \cdot \exp\left(\frac{-E/R}{T+273}\right) \tag{3}$$

where α and β are numerical exponential parameters for evaluation. By adding the actual values of k_b, TOC, Cl_0, and temperature listed in Table 3 to Eq. (3), the value of α and β was established based on the value of $-E/R$ obtained from above results.

Table 3
Chlorine decay rate coefficients and parameter solution in Eq. (2)

Waters	ICC (mg/L)	Temperature (℃)	DOC (mg/L)	Overall k (h^{-1})	k_b (h^{-1})	Δk (h^{-1})	$-E/R$ (℃)	F
Municipal water	0.4	10	5.87 ± 0.14	1.137	0.716	0.421	6,110	1.7×10^9
	0.4	20		2.622	1.496	1.126		
	3.5	10		0.068	0.024	0.044	5,918	2.9×10^8
	3.5	20		0.106	0.049	0.057		
NF permeate	0.4	10	2.67 ± 0.03	0.609	0.245	0.364	5,679	1.3×10^9
	0.4	20		1.066	0.486	0.580		
	3.5	10		0.110	0.019	0.091	5,526	5.7×10^6
	3.5	20		0.168	0.037	0.131		

For municipal water, the values of α and β of Eq. (3) yields Eq. (4):

$$k_b = \mathrm{TOC}^{11.04} \cdot \mathrm{Cl}_0^{-1.88} \cdot \exp\left(\frac{-E/R}{T+273}\right) \quad (4)$$

For NF permeate, the values of α and β yields Eq. (5):

$$k_b = \mathrm{TOC}^{17.67} \cdot \mathrm{Cl}_0^{-1.43} \cdot \exp\left(\frac{-E/R}{T+273}\right) \quad (5)$$

3.2.2. *Application of other models of chlorine decay in bulk waters*

In the past several decades, many researchers investigating chlorine disappearance in drinking water in several countries, have proposed a number of models to describe the decay kinetics of chlorine. In order to improve on the simple first-order model of chlorine decay, other studies proposed several more robust kinetic laws. Seven bulk chlorine decay kinetic models were reviewed and integrated (Table 4).

Figs. 5 and 6 present model fittings of the bulk chlorine decay in NF permeate for the models detailed in Table 4. The seven models closely represented on the feature of chlorine decay when the ICC was 0.4 mg/L, based on the coefficient of determination (R^2) of the regression >0.91, with levels of significance of well below 0.001. However, when ICC was 3.5 mg/L, the first- and second-order models (chlorine only) failed to adequately fit the decay data, while the other models continued to perform well. The results are consistent with Vasconcelos et al.'s report [36].

3.2.3. *THM formation*

To investigate THM formation kinetics in desalinated seawater, four (two finished waters with two initial chlorine concentrations at a constant tempera-

Table 4
Bulk chlorine decay kinetic models (refined from Vieira et al. [36,37])

Model forms	Formula	Refs.
Limited first-order	$C_t = C^* + (C_0 - C^*) \cdot \exp(-k_b t)$	[38]
Parallel first-order	$C_t = C_0 \cdot z \cdot \exp(-k_{\mathrm{bfast}} t) + C_0 \cdot (1-z) \cdot \exp(-k_{\mathrm{bslow}} t)$	
nth order	$C_t = \left[k_b(n-1) + C_0^{-(n-1)}\right]^{-1/(n-1)}$	
Combined first- and second-order model	$\frac{1}{C_t} + \frac{k_2}{k_1} = (\frac{1}{C_0} + \frac{k_2}{k_1}) \cdot \exp(k_1 t)$	[33]
Second-order (with respect to chlorine only)	$C_t = \frac{C_0}{1 + C_0 k_b t}$	[39]
Second order (with respect to chlorine and another reactant)	$C_t = \frac{C_0(1-R)}{1 - R\exp(-ut)}$	[32,40]
Parallel second-order model	$C_t = \frac{C_{\mathrm{clFRA}}(t) - c}{1 - \frac{c}{C_{\mathrm{clFRA}}(t)} \cdot \exp(-(C_{\mathrm{clFRA}}(t) - c) \cdot k_{\mathrm{clSRA}} t)}$	[39]

Note: Where C_0 is ICC, k_b is the bulk decay coefficient.

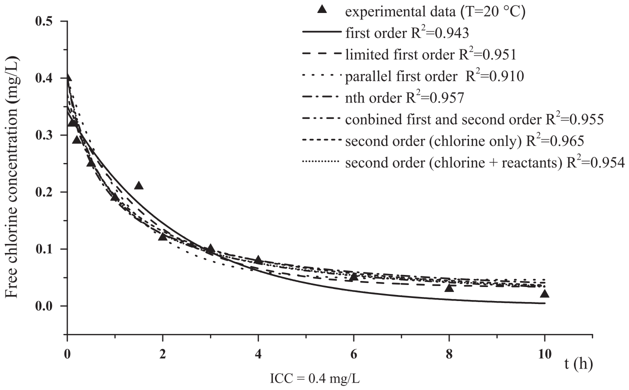

Fig. 5. Bulk chlorine decay fitting in NF permeate with ICC = 0.4 mg/L.

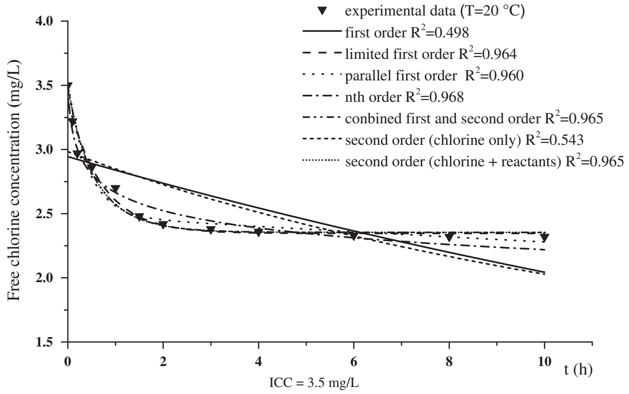

Fig. 6. Bulk chlorine decay fitting in NF permeate with ICC = 3.5 mg/L.

ture of 20℃) sets of data were obtained from laboratory experiments. Another four data-sets were obtained from field experiments using the pilot-scale DWDS to determine its effects on the THM formation.

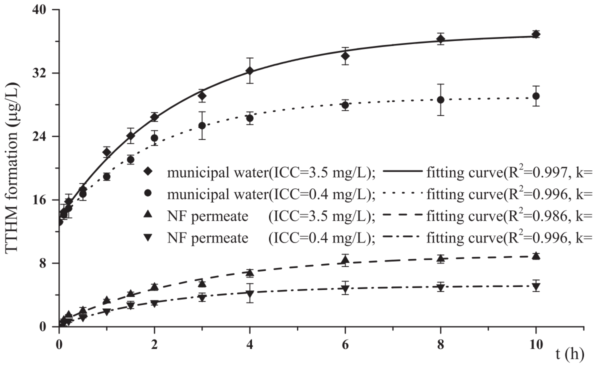

Fig. 7. TTHM formation vs. time for experiments in municipal water and NF permeate.

3.2.3.1. *TTHM formation kinetic.* The laboratory experimental data of THM formation were fitted to the first-order model. TTHM formation curves for experiments conducted on municipal water and NF permeate are presented in Fig. 7. In all cases, the coefficient of determination (R^2) of the regressions were >0.98 with levels of significance of well below 0.001. The first-order growth coefficients are also presented in Fig. 7.

The initial TTHM concentrations in the NF permeate and municipal water were 0 and 13.17 ± 0.21 μg/L (containing TCM: 9.49, BDCM: 3.17, DBCM: 0.51, TBM: 0 μg/L), respectively. Such initial TTHM in the municipal water already existed before pumping into the DWDS. Agus et al. [42] reported that the TTHM formed during chlorination of seawater would depend on the concentration and nature of the DOC precursors. The incremental yield of TTHM formed per mole of DOC in the NF permeate and municipal water at 10 h were 3.32 and 4.03 μg/mg, respectively, when the ICC was 3.5 mg/L; while 1.93 and 2.71 μg/mg were formed when the ICC was 0.4 mg/L. Higher DOC concentration would increase the chlorine demand and TTHM formation. The initial concentration would also increase the TTHM/DOC formation (TTHM formation per DOC, μg/mg) with the increase in chlorine dosage. As shown in Fig. 7, the TTHM/DOC formation increased by 72.0% and by 48.7% in the NF permeate and municipal water, respectively, when the ICC increased from 0.4 to 3.5 mg/L. The results suggest that high-DOC water source and high ICC would largely increase the THM formation.

3.2.3.2. *Relationship between measured TTHM formation and chlorine demand.* The relationship between TTHM formation and chlorine demand was evaluated from

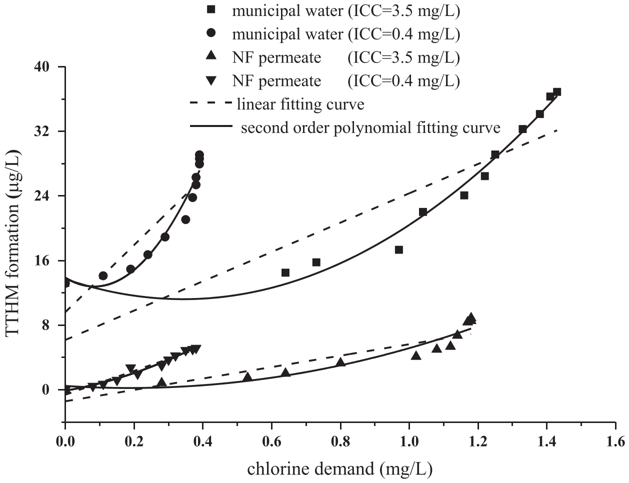

Fig. 8. Relationship between measured TTHM formation and chlorine demand.

Table 5
Fitting curves between TTHM formation and chlorine demand

Water samples	Linear	Second-order polynomial
Calibrated model	$y = Ax + B$	$y = ax^2 + bx + c$
Municipal water; ICC = 3.5 mg/L	$y = 18.15x + 6.18$ (0.74)	$y = 21.28x^2 - 14.57x + 13.71$ (0.98)
Municipal water; ICC = 0.4 mg/L	$y = 7.06x - 1.43$ (0.80)	$y = 7.45x^2 - 2.77x + 0.48$ (0.89)
NF permeate; ICC = 3.5 mg/L	$y = 41.55x + 9.62$ (0.80)	$y = 153.97x^2 - 26.00x + 13.89$ (0.94)
NF permeate; ICC = 0.4 mg/L	$y = 14.76x - 0.61$ (0.95)	$y = 18.17x^2 - 7.31x - 0.11$ (0.97)

Notes: Numbers in parentheses = R^2; y = TTHM formation (μg/L) and x = chlorine demand (mg/L).

residual chlorine and TTHM data for both the NF permeate and municipal water. Four data-sets from laboratory experiments were used and relationship curves are shown in Fig. 8, and curve parameters are detailed in Table 5.

It can be seen from Fig. 8 that the linear and second-order polynomial curves fitted describe the relationship between TTHM formation and chlorine demand. Table 5 shows the calibrated models for the two waters, as well as the estimated model parameters and the coefficient of determination (R^2) of the regression.

Many studies [7,32,36,41,43] have been reported which explored the relationship between the THM formation and chlorine demand. Clark [41] proposed a second-order model which links the THM formation with chlorine demand and the maintenance of chlorine residuals in drinking waters. Boccelli et al. [32] reported that a linear relationship between TTHM formation and chlorine demand is appropriate under both single dose and rechlorination conditions based on the high-linear correlation coefficients. He attributed the differences of model parameters to the diversity of chemicals in waters and presence or absence of THM formed from previous disinfection treatments. However, the work reported here is not consistent with that of Boccelli et al. [32]. Form Fig. 8, it can be seen that the second-order fitting curve better describe the relationship between TTHM formation and chlorine demand (see Table 5). These results support the work by Rodrigues et al. [43], in which the factorial analysis was conducted on THM formation in water following chlorine addition. In their work, numerical models of the relationship between THM formation and impacting factors including chlorine were proposed.

4. Conclusions

Desalinated seawater is an important water resource for drinking water supply. However, potential microbial and chemical risks from desalinated seawater chlorination and its mechanism of chlorine decay and DBPs formation in the DWDS have received little attention.

In this study, seawater desalinated by UF and NF membranes was pumped into a pilot-scale DWDS. Chlorine was added in the form of sodium hypochlorite. The characteristics of NF permeate and municipal waters were determined and compared. The NF permeate was of lower DOC concentration than municipal water, and the fluorescence intensity of protein-like NDOM in municipal water sample was more than 20 times that of NF permeate sample.

Based on the characteristics of the two finished waters, chlorine decay and THM formation were evaluated. Free chlorine, DOC concentration and species (in the aspects of protein-like and humic-like matters), and temperature are the factors that can affect chlorine decay and THM formation.

A first-order model was applied to evaluate chlorine decay of desalinated seawater. A new model combining ICC, DOC concentration, and temperature was developed and first-order decay coefficients were determined. Seven other models describing the kinetics of chlorine decay were also applied and compared in this study.

TTHM formation kinetics were studied and a first-order model is suggested to describe this formation. TTHM concentration and first-order growth coefficients in municipal water are higher than that in NF permeate. TTHM/DOC formation also largely increased with the increasing chlorine dosage.

The relationship between TTHM formation and chlorine demand was demonstrated. The results showed that a second-order polynomial model is better than a linear model. More experiments with respect to the microbial and chemical risks are suggested to investigate the safety of transporting desalinated seawater into the DWDS.

Acknowledgments

This work was supported in part by the National Natural Science Foundation of China (Grant No. 51208455), Research Fund for the Doctoral Program of

Higher Education of China (Grant No. 20110101120033), the National Major Program on Pollution Control and Management of Water Body (Grant No. 2012ZX07403-003), and the Program for Zhejiang Leading Team of S&T Innovation (2010R50037).

References

[1] Q. Schiermeier, Water: Purification with a pinch of salt, Nature 452 (2008) 260–261.

[2] M. Elimelech, W.A. Phillip, The future of seawater desalination: Energy, technology, and the environment, Science 333 (2011) 712–717.

[3] A.D. Khawaji, I.K. Kutubkhanah, J.M. Wie, Advances in seawater desalination technologies, Desalination 221 (2008) 47–69.

[4] L.F. Greenlee, D.F. Lawler, B.D. Freeman, B. Marrot, P. Moulin, Reverse osmosis desalination: Water sources, technology, and today's challenges, Water Res. 43 (2009) 2317–2348.

[5] C. Diawara, M. Rumeau, D. Aureau, P. Hemmery, Seawater nanofiltration (NF): Fiction or reality? Desalination 158 (2003) 277–280.

[6] P. Biswas, C. Lu, R.M. Clark, A model for chlorine concentration decay in pipes, Water Res. 27 (1993) 1715–1724.

[7] L.A. Rossman, R.M. Clark, W.M. Grayman, Modeling chlorine residuals in drinking-water distribution systems, Nature 120 (1994) 803–820.

[8] O. Wable, N. Dumoutier, J.P. Duguet, P.A. Jarrige, G. Gelas, J.F. Depierre, Modeling chlorine concentrations in a network and applications to Paris distribution network, Proc. Water Quality Modeling in Distribution Systems, AWWA Research Foundation, US EPA, Cincinnati, OH, 1991.

[9] I. Fisher, G. Kastl, A. Sathasivan, Evaluation of suitable chlorine bulk-decay models for water distribution systems, Water Res. 45 (2011) 4896–4908.

[10] M. Deborde, U. von Gunten, Reactions of chlorine with inorganic and organic compounds during water treatment—Kinetics and mechanisms: A critical review, Water Res. 42 (2008) 13–51.

[11] M.J. Nieuwenhuijsen, M.B. Toledano, N.E. Eaton, J. Fawell, P. Elliott, Chlorination disinfection byproducts in water and their association with adverse reproductive outcomes: A review, Occup. Environ. Med. 57 (2000) 73–85.

[12] S.D. Richardson, M.J. Plewa, E.D. Wagner, R. Schoeny, D.M. Demarini, Occurrence, genotoxicity, and carcinogenicity of regulated and emerging disinfection by-products in drinking water: A review and roadmap for research, Mutat. Res./Rev. Mutat. Res. 636 (2007) 178–242.

[13] W.D. King, L.D. Marrett, C.G. Woolcott, Case-control study of colon and rectal cancers and chlorination by-products in treated water, Cancer Epidemiol. Biomarkers Prev. 9 (2000) 813–818.

[14] M.E. Hildesheim, K.P. Cantor, C.F. Lynch, M. Dosemeci, J. Lubin, M. Alavanja, G. Craun, Drinking water source and chlorination byproducts II. Risk of colon and rectal cancers, Epidemiology 9 (1998) 29–35.

[15] C.M. Villanueva, K.P. Cantor, S. Cordier, J.J. Jaakkola, W.D. King, C.F. Lynch, S. Porru, Disinfection byproducts and bladder cancer, Epidemiology 15 (2004) 357–367.

[16] S.W. Krasner, H.S. Weinberg, S.D. Richardson, S.J. Pastor, R. Chinn, M.J. Sclimenti, G.D. Onstad, Occurrence of a new generation of disinfection byproducts, Environ. Sci. Technol. 40 (2006) 7175–7185.

[17] E.P.A. Us, National primary drinking water regulations: Disinfectants and disinfection byproducts-final rule, Fed. Reg. 63 (1998) 69390.

[18] WHO, 2006, (accessed on March 11, 2015). Available from: <http://www.who.int/water_sanitation_health/dwq/gdwq0506.pdf>.

[19] Ministry of Health of People's Republic of China, Standards for Drinking Water Quality (GB 5749-2006), Beijing, 2006, p. 12.

[20] X.C. Li, C. Li, Y.L. Yang, X.W. Mao, Performance evaluation of common household water filters in China, Fresenius Environ. Bull. 23 (2014) 2460–2465.

[21] C. Li, Y.J. Yang, J.Z. Yu, T.Q. Zhang, X.W. Mao, W.Y. Shao, Second-order chlorine decay and trihalomethanes formation in a pilot-scale water distribution systems, Water Environ. Res. 84 (2012) 656–661.

[22] J. Świetlik, E. Sikorska, Application of fluorescence spectroscopy in the studies of natural organic matter fractions reactivity with chlorine dioxide and ozone, Water Res. 38 (2004) 3791–3799.

[23] S. Platikanov, R. Tauler, P.M. Rodrigues, M.C.G. Antunes, D. Pereira, J.C.E. da Silva, Factorial analysis of the trihalomethane formation in the reaction of colloidal, hydrophobic, and transphilic fractions of DOM with free chlorine, Environ. Sci. Pollut. Res. 17 (2010) 1389–1400.

[24] P.G. Coble, Characterization of marine and terrestrial DOM in seawater using excitation–emission matrix spectroscopy, Mar. Chem. 51 (1996) 325–346.

[25] J. Chen, E.J. LeBoeuf, S. Dai, B. Gu, Fluorescence spectroscopic studies of natural organic matter fractions, Chemosphere 50 (2003) 639–647.

[26] C.A. Stedmon, R. Bro, Characterizing dissolved organic matter fluorescence with parallel factor analysis: A tutorial, Limnol. Oceanogr. Methods 6 (2008) 572–579.

[27] C.A. Stedmon, S. Markager, R. Bro, Tracing dissolved organic matter in aquatic environments using a new approach to fluorescence spectroscopy, Mar. Chem. 82 (2003) 239–254.

[28] P.G. Coble, S.A. Green, N.V. Blough, R.B. Gagosian, Characterization of dissolved organic matter in the Black Sea by fluorescence spectroscopy, Nature 348 (1990) 432–435.

[29] P.G. Coble, C.E. Del Castillo, B. Avril, Distribution and optical properties of CDOM in the Arabian Sea during the, Southwest Monsoon, Deep-Sea Res. Part II-Top. Stud. Oceanogr. 45 (1998) 2195–2223.

[30] N.V. Blough, R. Del Vecchio, Chromophoric DOM in the coastal environment, Biogeochem. Mar. Dissolved Org. Matter (2002) 509–546.

[31] N.B. Hallam, F. Hua, J.R. West, C.F. Forster, J. Simms, Bulk decay of chlorine in water distribution systems, Water Res. 129 (2003) 78–81.

[32] D.L. Boccelli, M.E. Tryby, J.G. Uber, R.S. Summers, A reactive species model for chlorine decay and THM formation under rechlorination conditions, Water Res. 37 (2003) 2654–2666.

[33] R.M. Clark, M. Sivaganesan, Predicting chlorine residuals in drinking water: Second order model, Water Res. 128 (2002) 152–161

[34] F. Hua, J.R. West, R.A. Barker, C.F. Forster, Modelling of chlorine decay in municipal water supplies, Water Res. 33 (1999) 2735–2746.

[35] J.C. Powell, N.B. Hallam, J.R. West, C.F. Forster, J. Simms, Factors which control bulk chlorine decay rates, Water Res. 34 (2000) 117–126.

[36] J.J. Vasconcelos, P.F. Boulos, Characterization and Modeling of Chlorine Decay in Distribution Systems, American Water Works Association, Denver, CO, 1996, p. 405.

[37] J.C. Powell, J.R. West, N.B. Hallam, C.F. Forster, J. Simms, Performance of various kinetic models for chlorine decay, J. Water Resour. Planning Manage. 126 (2000) 13–20

[38] P. Vieira, T. Coelho, D. Loureiro, Accounting for the influence of initial chlorine concentration, TOC, iron and temperature when modelling chlorine decay in water supply,, Aquaculture 53 (2004) 453–467.

[39] C.N. Haas, S.B. Karra, Kinetics of wastewater chlorine demand exertion, Chem. Eng. J. 56 (1984) 170–173

[40] A. Jabari Kohpaei, A. Sathasivan, Chlorine decay prediction in bulk water using the parallel second order model: An analytical solution development, Chem. Eng. J. 171 (2011) 232–241.

[41] R.M. Clark, Chlorine demand and TTHM formation kinetics: A second-order model, Anal. Chim. Acta 124 (1998) 16–24.

[42] E. Agus, N. Voutchkov, D.L. Sedlak, Disinfection by-products and their potential impact on the quality of water produced by desalination systems: A literature review, Desalination 237 (2009) 214–237.

[43] P.M. Rodrigues, J.C. Esteves da Silva, M.C.G. Antunes, Factorial analysis of the trihalomethanes formation in water disinfection using chlorine, Anal. Chim. Acta 595 (2007) 266–274.